https://doi.org/10.5194/hess-2024-48
Preprint. Discussion started: 26 February 2024

Hydrology and Earth System Sciences
Open Access
Discussions

Future drought over Urmia Lake Basin under SSP scenarios: the relevance of snow melt

Maral Habibi[1,*], Iman Babaeian[2], Wolfgang Schöner[1]
[1] Department of Geography and Regional Science, University of Graz, 8010 Graz, Austria
[2] Climate Research Institute, Research Institute for Meteorology and Atmospheric Science, Mashhad 91735-676, Iran
Correspondence to: M. Habibi (Maral.habibi@uni-graz.at)

Abstract

Snow melt is one of the sources of freshwater supply in the late spring and summer in the mountainous regions of Iran, especially in the Urmia Lake Basin (ULB). In this study, past and future droughts of Urmia Lake Basin (ULB) have been studied by analyzing three types of droughts: (I) precipitation-deficit based characterized by the Standardized Precipitation Index (SPI), (ii) precipitation-evapotranspiration based droughts characterized by the Standardized Precipitation and Evapotranspiration Index (SPEI) and (iii) those droughts forced additionally by snow melt using the Snowmelt and Rain Index (SMRI). While reanalysis data ERA5-land describes the past climate, bias-corrected CMIP6 ensemble serves as the data for the future climate. Contrary to the SPI drought index, an increasing trend has been projected both in snowmelt-based (SMRI trend -0.068 units/year) and evapotranspiration-based (SPEI trend -0.079 units/year) drought indices, both for the period 1995-2014 and significant at the 5% level. This indicates that summer droughts in the ULB will increase in the future, particularly because of increasing evapotranspiration and less snowmelt, while precipitation changes play a minor role.

Drought severity will increase from the near future (2021-2040) to the far future (2081-2100), particularly forced by snowmelt deficit under the SSP5-8.5 scenario for the far future. Under the present climate, the extent of drought-affected areas is similar for all three types of droughts. However, under future climate drought-affected areas forced by snowmelt deficit will increase from about 20% in the near future (2021-2040) to 60% in the far future (2081-2100), showing that snow melt plays a vital role in aggravating the drought over the Basin. A

https://doi.org/10.5194/hess-2024-48
Preprint. Discussion started: 26 February 2024

Hydrology and Earth System Sciences
Discussions

decrease in the Basin's drought trend in the 2080s and later can be seen both for SMRI and SPEI indices under SSP1-2.6, which may be due to the temperature effect on snowmelt and evapotranspiration from the reduction of greenhouse gas emissions in SSP1-2.6 scenario at the end of 21st century. Such a decrease in SMRI and SPEI drought indices can also be seen around the 2090s under the SSP2-4.5 scenario. Results also reveal that the mountainous areas of the Basin will experience much less drought compared to the lowlands (including the lake) and foothills.

Keywords: Climate change, future drought, drought indices, mountains, snow droughts, Urmia Lake, Iran

1. Introduction

Human-induced climate change has emerged globally in temperature and evapotranspiration increases and precipitation changes. These changes significantly impact hydrometeorological disasters, including droughts, floods, heat waves, and others (Cowherd et al., 2023; An et al., 2022; IPCC, 2021; Sharma et al., 2021; Separated & Nafung, 2021; Bazaz et al., 2018; Huo-Po et al., 2013). Drought is a complex and costly natural disaster that is difficult to monitor and define. One difficulty is that drought has different meanings in different regions and occurs in areas with high and low precipitation. Above-normal temperatures increase the atmospheric water demand, increasing the evapotranspiration and lowering the total water availability and resultant streamflow. In mountain regions, snow plays an additional role. Snow-based droughts are rapidly increasing and are expected to accelerate over the next several decades in many regions worldwide due to changes in snow cover from anthropogenic climate change (Hunting & Hauschka, 2020). In such cases, cascading effects can result, extending from mountains to lowlands with associated impacts on human livelihood, economy, and ecosystems (Wilhite & Glantz, 1985; Mondal et al., 2023; Andreadis et al., 2005; Sheffield et al., 2012; Mokhtari & Akhoondzadeh, 2021; Huss et al., 2017). Snow-based droughts have to be distinguished from winter droughts, which are also

https://doi.org/10.5194/hess-2024-48
Preprint. Discussion started: 26 February 2024

related to snow but followed by missing snow melts in winter. Such droughts, quite common in mountain regions, will decrease from future climate change (Parka et al., 2016).

Several previous studies have assessed snow-based droughts by snowmelt-based drought indices at different scales and scenarios in different regions and climates worldwide. Most of these studies focused on catchments with near-normal flow that are minimally impacted by water management. According to Rhoades et al. (2022), preventing a low-to-no-snow future in either hemisphere requires global warming to be held to, at most, +2.5 °C. CMIP6 simulations pinpoint snow drought as an emerging global threat to water resources and highlight the need to explore higher-resolution future models that better capture complex mountain topography, wildland fires, and snow-forest interactions (Cowherd et a., 2023). Staudinger et al. (2014) compared SPI, SSI (Standard stream flow index), and SMRI drought indices for seven Swiss catchments with different contributions of snowmelt to streamflow and showed that the SMRI improves the description of hydrological droughts for snow-dominated basins. In an earlier study, Van Loon and Van Lanen (2012) proposed six different hydrological drought types for 21 catchments in Austria and Norway based on governing drought propagation processes derived from catchment-scale drought analysis (classical rainfall deficit drought, rain-to-snow-season drought, wet-to-dry-season drought, cold snow season drought, warm snow season drought, and composite drought). The most common drought type in all European catchments was the classical rainfall deficit drought (almost 50% of all events). If only the five most severe drought events of each catchment are considered, a shift towards more rain-to-snow-season shortages, warm snow-season droughts, and composite droughts was found. Myers et al. (2023) used the Soil and Water Assessment Tool (SWAT) hydrologic model to study Rain-On-Snow (ROS) melt events in a warming climate in the North American Great Lakes Basin for 1960–2069. Whereas warmer, southern sub-basins show an approximately 30 % reduction in snowmelt in mid-century (2040–2069) due to changes in ROS events, colder, northern subbasins are characterized by a 5% reduction in snowmelt. Berghuis et al. (2014) demonstrated that in catchments of the

https://doi.org/10.5194/hess-2024-48
Preprint. Discussion started: 26 February 2024

United States, a higher fraction of precipitation falls as snow is associated with higher mean streamflow compared to catchments with marginal or no snowfall.

In Asia, between 1979-99 and 1999-2019, "snow meltwater supply" to rivers in high-mountain areas dropped by an average of 16%. Meanwhile, an extremely high future warming scenario would drive a 40% drop in snow meltwater supply (Kraaijenbrink, 2021). The snowmelt runoff model (SRM) coupled with MODIS remote sensing data and the scenarios of precipitation and temperature from the regional climate model PRECIS were employed to study future discharges in the Karakoram Range of Pakistan. The increase of 3 °C in mean annual temperature by the end of the 21st century may result in an accumulation of 35–40% in Gilgit River flows. Future climate change scenarios indicate a doubling of summer runoff until 2075 (Adnan et al., 2017; Ahmad Tahir et al., 2011). Hunting and Hauschka (2020) showed that the duration of snow drought in the Hindu Kush and Central Asia experienced decreases by −4 and −7%, respectively, during the second half of 1980-2018, compared to the first half of the period. Iran has a diverse climate, so about 15% of Iran's area has a semi-humid to humid climate, 55% is semi-arid, and about 30% is an arid and hyper-arid climate. Iran's average precipitation is 235 mm, and the average temperature is 19.1 degrees from 1987 to 2017. Its average precipitation decreases by 2.1 mm/yr., while its average temperature increases by 0.05oC/yr., which is significant with a 0.95 confidence level (Abbasi et al., 2019). The Urmia long-term average annual temperature is 12.3oC. Long-term average evaporation (1966-2000) from Lake Urmia is 1374 mm/yr. Precipitation in the Urmia basin is estimated to be 303 mm/yr., falling from October to March, with the highest amount in spring (Alizadeh-Choobari, 2016). Its climate has changed from humid during the reference period of 1961-1990 to semi-arid in the most recent decade of 1993-2022 based on the UNEP aridity index.

In Iran, snow droughts still need to be explored compared to other types of droughts, and studies addressing snow droughts are rare. One of the first steps towards understanding the relevance of snow droughts by the example of ULB was done by Habibi et al. (2021), who analyzed drought characteristics over ULB by three types of drought indices including SPI

https://doi.org/10.5194/hess-2024-48
Preprint. Discussion started: 26 February 2024

Hydrology and Earth System Sciences Discussions

(Standardized Precipitation Index), SPEI (Standardized Precipitation-Evaporation Index) and SMRI (Snow Melt Rain Index) over 1981-2018. The results show intensified SPEI and SMRI droughts in the most recent decades, but usually, no notable change has been detected for SPI. Also, no significant snow-based drought (described by SMRI) was detected before 1995, indicating sufficient availability of snowfall in the Basin at that time. Above-average temperatures in the year result in earlier snowmelt and, therefore, an earlier streamflow peak. This may result in streamflow droughts later in the year when the snowmelt peak is expected (Vicente-Serrano et al., 2014) and confirmed for ULB by Saboor and Mir Mousavi (2014), who showed a significant decline in snowfall for most of the meteorological stations in the Basin. Precipitation is less likely to occur in a warmer climate as snow falls, leading to more frequent snow droughts with vigorous intensity and longer duration. However, societies and ecosystems within and downstream of the mountain's region rely on seasonal snowmelt to satisfy their water demands in the Urmia Lake region.

Drought indices are a widely used method for assessing droughts. They model meteorological, agricultural, hydrological, and socioeconomic drivers of droughts, depending on the analytical approach, by limited input variables such as precipitation, air temperature, runoff, soil moisture, and snowmelt (Supharatid & Nafung, 2021; Kim et al., 2020). Index-based methods benefit from their lower data and computational requirements while achieving a higher degree of modeling success than distributed hydrological modeling efforts. While precipitation-based drought indices, such as the Standardized Precipitation Index (SPI), are widely used for drought monitoring and early warning, the adverse consequences of drought are limited to not only the lack of precipitation but also other hydroclimatic drivers, such as soil/groundwater, evapotranspiration, and snow melt (Tijdeman et al., 2018; Van Loon et al., 2015). In a recent study, Laimighofer and Laaha (2022) showed for both SPI and SPEI that the choice of distribution and observational window have a relevant impact on the index values and, thus, the uncertainty of drought assessment. The PET calculation for SPEI introduces additional uncertainty. So, absolute values of the indices have to be treated with care and seen as a first-guess estimate of droughts.

https://doi.org/10.5194/hess-2024-48
Preprint. Discussion started: 26 February 2024

Hydrology and Earth System Sciences Discussions

The focus of this study is to analyze future changes in droughts for the ULB in Iran until 2100. Given the results from previous studies, a particular focus is given to changes in snow droughts, which are separated from precipitation deficit droughts and precipitation-evaporation droughts. Different drought indices and related drought severity, duration, and frequency measures characterize these droughts. To describe the future climate for the study region bias, corrected CMIP6 model simulations under different SSP scenarios are used. Based on this modeling frame, spatial drought patterns for the near, mid, and far future and their causes for the ULB are shown.

2. Methodology

2.1 Study area

The study area of this research is Urmia Lake Basin (ULB), with an area of about 52000 km² located in East and West Azerbaijani and Kurdistan provinces in the northwest of Iran. Its western border is the border between Iran and Turkey. Lake Urmia is the world's second-largest saline lake, and its main rivers, Abishai, Zarinerood, and Siminerood, are essential to the basin-wide water cycle. The elevation range covers the highest elevation of the basin at Sablan with an elevation of 4811 m.a.s.l. Up to the basin's lowest part, Urmia Lake at 1280 m.a.s.l. (Fig 1). The Mediterranean climate of the ULB is influenced by the surrounding high mountains and is characterized by cold winters and relatively temperate summers. The basin's annual average temperature is 12.3°C, precipitation is about 303mm, and average evaporation is about 1374 mm from 1966-2000. The basin's precipitation falls from October to March, with the highest amount in spring (Habibi et al., 2021; Alizadeh-Choobari, 2018; Abbasi et al., 2019).

https://doi.org/10.5194/hess-2024-48
Preprint. Discussion started: 26 February 2024

Hydrology and Earth System Sciences
Discussions
Open Access

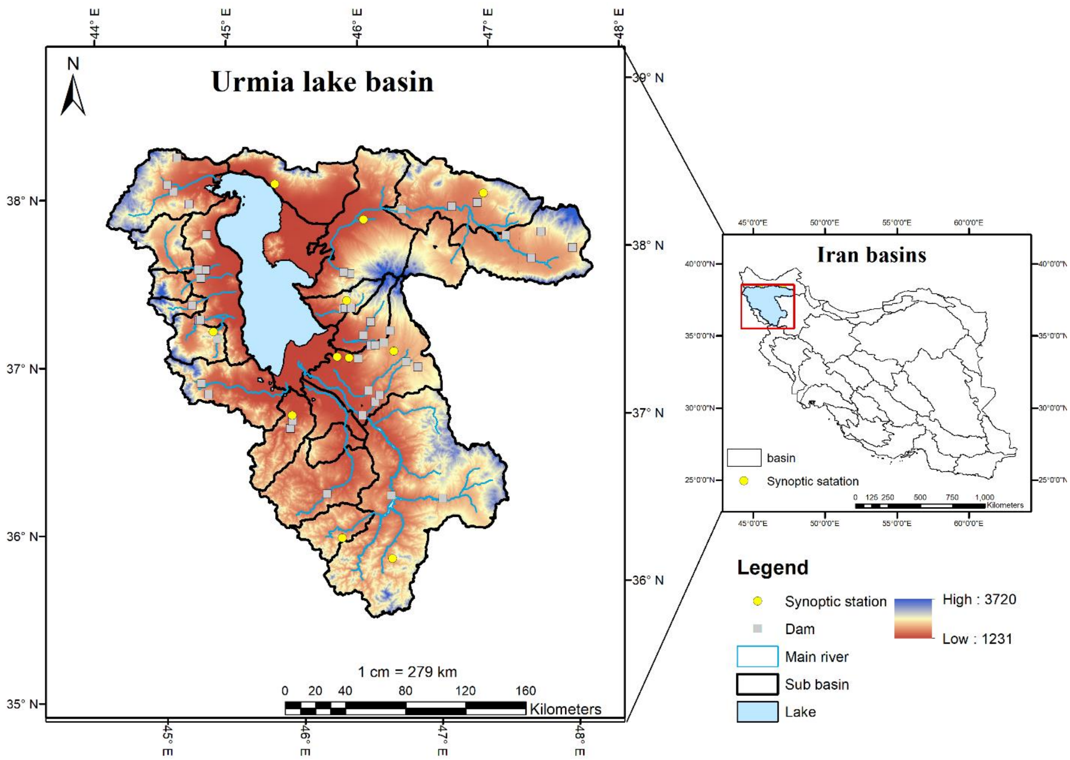

Figure 1. Geographical location of Lake Urmia.

2.2 Data

Three types of data have been used in this study. The first is grided precipitation, temperature, and snow depth reanalysis data from ERA5-land. ERA5-Land data has a spatial resolution of approximately 9 km. This high-resolution dataset provides hourly information on surface variables, making it suitable for various land surface applications. The skill of ERA5-land data has been confirmed globally and over Iran by many researchers (Muñoz-Sabater, 2021; Sam et al., 2022; Ghajarnia et al., 2022; Izadi et al., 2021). The second data is CMIP6 model data under SSP scenarios. To simulate the future drought of the basin, CMIP6 models have been used. As the first step in the selection of the models, CMIP6 models were

https://doi.org/10.5194/hess-2024-48
Preprint. Discussion started: 26 February 2024

screened based on the availability of daily precipitation, snowfall, and minimum and maximum temperature, both in historical and future periods under three scenarios of SSP1-2.6, SSP2-4.5, and SSP5-8.5. CMIP6 has a similar or even slightly higher skill in reproducing historical large-scale mean surface temperature and precipitation patterns than previous CMIP models used to prepare IPCC circular assessment reports (Bock et al., 2020). Likewise, Chen et al. (2020) notes a general improvement of CMIP6 in the simulation of climate extremes and their trend patterns compared to observations. Table 1 shows the model's name, resolution, description, and data citations of the screened models. The most critical limitation in the selection of CMIP6 models was accessibility to their monthly data both for historical and future periods under three optimistic (SSP1-2.6), medium (SSP2-4.5), and pessimistic (SSP5-8.5) scenarios and the third dataset was observational data as it has also been used in our previous study (Habibi et al., 2021).

2.3 Bias correction

In our study, we employed a range of bias correction techniques to enhance the accuracy of our climatological and hydrological models. The Delta Method (DELTA) involves simple adjustments to the model outputs by adding the mean difference between observed and modeled data, offering a straightforward correction. Empirical Quantile Mapping (EQM) aligns the cumulative distribution function of the model outputs with that of observed data, catering to the entire data distribution. For more intricate adjustments, Generalized Quantile Mapping (GQM) allows complex modifications to model data distributions, enhancing alignment with observational data. Parametric Transformations (PTF) involve fitting parametric functions to the quantile-quantile relation of observed and modeled data, aiding in effective distribution matching. Non-parametric quantile Mapping (QUANT) estimates and applies empirical cumulative distribution functions at regular quantiles to correct model data. Robust Quantile Mapping (RQUANT) employs local linear regression for a robust approach to quantile-quantile estimation, which is particularly useful in handling outliers. The Scale Method provides a simple, yet effective scaling of model data based on the ratio of observed to modeled data means. Lastly, Smoothing Spline Quantile Mapping (SSPLIN)

https://doi.org/10.5194/hess-2024-48
Preprint. Discussion started: 26 February 2024

utilizes smoothing splines fitted to quantile-quantile plots for adjusting model data distributions, ensuring a closer match to observed data.

Table 1. List of selected CMIP6 model with their ECS and atmospheric resolution used in this study for historical and SSP1-2.6, SSP2-4.5, and SSP5-8.5 experiments.

Model	Institution	Country	ECS (° C)	Resolution	Citation
CMCC-ESM2	CMCC	Italy	3.6	100 km	Lovato et al (2022)
EC-Earth3-Veg	EC-Earth	Consortium (Europe)	4.3	250 km	EC-Earth (2019)
EC-Earth3	EC-Earth		4.3	100 km	EC-Earth (2019)
Nor-ESM2-MM	NorESM	Norway	2.5	100 km	Bentsen et al (2019)
TAI-ESM1	TAI-ESM	Taiwan	4.3	100 km	Lee et al (2020); Yi-Chi et al (2022)
MRI-ESM-2.0	MRI	Japan	4.0	100 km	Yukimoto et al (2019a, 2019b, 2019c)
GFDL-ESM4	NOAA	USA	5.0	100 km	Guo et al (2018a, 2018b, 2018c)

ERA5 data has been used to evaluate CMIP6 model simulation in the historical period. ERA5 is the latest climate reanalysis data produced by the European Center for Medium-range Weather Forecast (ECMWF), providing hourly to annual time scale data on many atmospheric, land-surface, and sea-state parameters (Hersbach, 2020). The performance of these data in simulating meteorological variables over Iran has been studied and confirmed by many studies (Izadi et al., 2021; Kaviani Malayeri et al., 2021; Sam et al., 2022). To study the model's performance, pseudo-observation/reanalysis data from ERA5 of precipitation, snowfall, and minimum and maximum temperature were used for 1995-2014.

https://doi.org/10.5194/hess-2024-48
Preprint. Discussion started: 26 February 2024

2.4 Drought indices

In this study, we focused on three drought indices of SPI (McKee et al., 1993), SPEI (Vicente-Serrano et al., 2010), and SMRI (Staudinger et al., 2014). SPI assesses drought conditions based on long-term precipitation probability distribution. SPEI considers the differences between precipitation and potential evapotranspiration, using a log-logistic distribution. SMRI is based on precipitation and snowmelt minus snow accumulation.

SPI is defined as:

$$SPI_i = \frac{P_i - \bar{P}}{\sigma_P}$$

where P_i is the precipitation of the selected period during the year i, $\bar{P}$ is the long-term mean precipitation and σ_P is the standard deviation of precipitation for the set period. Precipitation data is transformed using the gamma distribution.

SPEI is defined as:

$$SPEI_i = P_i - PET_i$$

where P_i is the precipitation of the selected period for the year i, PET_i potential evapotranspiration of the selected period for year and $P_i - PET_i$ is the climatic water balance, which is transformed by log-logistic probability distribution.

$$PET_i = 1.6K\left(\frac{10Ti}{I}\right)^m$$

where T_i is the mean temperature of the selected period for the year i, I is the heat index calculated as the total of 12 monthly index values, m is a coefficient that depends on heat index and K is a factor of correction calculated as a function of the month and latitude.

https://doi.org/10.5194/hess-2024-48
Preprint. Discussion started: 26 February 2024

Hydrology and Earth System Sciences
Discussions

SMRI is defined as:

$$SMRI_i = P_i - PET_i + \sum_{i=1}^{\infty} SM - \sum_{i=1}^{\infty} SA$$

where *SM* is snow melt, *SA* is snow accumulation (both computed on a daily base), while $P_i - PET_i + \sum_{i=1}^{\infty} SM - \sum_{i=1}^{\infty} SA$ is the climatic water balance which is transformed by a Pearson type III distribution, using L-moments method for parameter estimation (see Staudinger et al., 2014 for details). Snow accumulation, expressed as the amount of liquid water accumulated as snow, occurs when mean temperature is below a threshold temperature of 1 °C, while snowmelt, expressed as the amount of liquid water melted, is calculated with a simple temperature index model using a melt factor of 3 mm °C-1 day-1 (similar to Staudinger et al., 2014).

Table 2 summarizes drought categories based on index values of the SPI, SPEI and SMRI, respectively.

Table 2. Drought classification

Drought category	**Class**
Moderate dryness	-1 to -1.49
Severe dryness	-1.5 to -1.99
Extreme dryness	<-2

https://doi.org/10.5194/hess-2024-48
Preprint. Discussion started: 26 February 2024

The indices described above allow us also to quantify drought severity (DS), and duration (DD), which are derived from the indices as described below.

The duration *(DD)* of drought is the period in which the SPEI/SPI/SMRI value is continuously negative. It starts when the indices values are equal to -1 and ends when values become positive. The drought severity *(S)* is the cumulated index values within the drought duration, which is defined by:

$$DS = -\sum_{i=1}^{DD} Indexes_i$$

2.5 Statistical tools

2.5.1. Taylor diagrams (Taylor, 2001) offer a visual framework for comparing sets of variables, typically obtained from one or more test data collections, with one or more reference data collections. Typically, the test data comprises model experiments, while the reference data is either a control experiment or reference observations. Taylor diagrams very usefully allow the visualization of the correlation and the root mean square error between test data and reference data as well as the standard deviations of both data sets at once.

2.5.2. Root Mean Square Error (RMSE) is a commonly used measure of the difference between a predicted value and the actual value. It is a square error loss function that penalizes larger errors more heavily than smaller errors. RMSE is calculated by taking the

https://doi.org/10.5194/hess-2024-48
Preprint. Discussion started: 26 February 2024

square root of the mean of the squared differences between the predicted values and the actual values.

$$RMSE = \sqrt{\sum_{i=1}^{i=n} \frac{(Pi - Oi)^{2^2}}{n}}$$

Where: n represents the total number of data points. P_i is the predicted value for the *itch* data point and O_i is the observed or reference value for the *itch* data point.

2.5.3. Normalized Root Mean Square Error (NRMSE) is a variant of RMSE that normalizes the error by the range of the actual values. This makes NRMSE more suitable for comparing the performance of different models on different datasets, as it is not affected by the scale of the data.

$$NRMSE = \frac{RMSE}{\max(y_i) - \min{(y_i)}}$$

where $\max(y_i)$ is the maximum value of the actual values, $\min(y_i)$ is the minimum value of the actual values. A lower RMSE or NRMSE indicates that the model is making more accurate predictions. An RMSE or NRMSE of 0 indicates that the model is perfectly predicting the actual values.

3. Results and discussion:

3.1 Bias correction

The model screening was the first step in the bias correction procedure of the models. In the second step, the performance of screened models for each variable was estimated against the ERA5-land gridded dataset (Muñoz-Sabater et al., 2021) based on the Taylor diagrams

https://doi.org/10.5194/hess-2024-48
Preprint. Discussion started: 26 February 2024

Hydrology and Earth System Sciences
Open Access
Discussions

and NRMSE indicator. Figure 2 shows the individual Taylor diagrams for annual precipitation, snow depth, and mean minimum and maximum temperature. From Taylor diagrams, it can be concluded that among all seven screened CMIP6 models, the Taisa, MRI-ESM2.0, NorESM2-MM, and MRI-ESM2.0 are the best-performing models in historical simulation of maximum temperature, minimum temperature, precipitation, and snowfall, respectively.

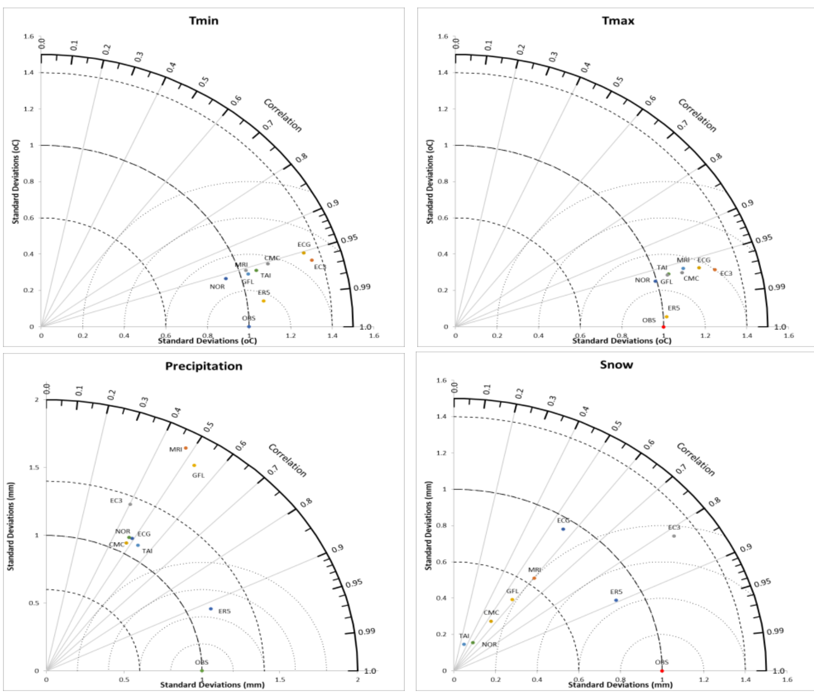

Figure 2. Performance of the CMIP6 models for annual precipitation totals, annual snow depth, mean minimum, and maximum temperature in comparison to observations (ERA5-Land) after bias correction for the ULB over the period 1995-2018 (Taylor diagrams)

https://doi.org/10.5194/hess-2024-48
Preprint. Discussion started: 26 February 2024

In the ultimate step in the bias correction procedure of the models used in this study, the bias of 4 selected models has been corrected using additive (temperature) and multiplicative (precipitation and snow depth) delta methods. Table 3 shows the Normalized RMSE (NRMSE) of raw and bias-corrected model data. Based on Despotovic et al. (2016), when NRMSE is used, model accuracy is excellent when NRMSE <10%, good if 10%<NRMSE<20%, fair 20%<NRMSE<30%, and poor if NRMSE>30%. Regarding the results shown in Table 3, the best-performing bias-corrected simulations belong to maximum temperature with an NRMSE value of 8.7%, which is categorized in the "excellent" category. Minimum temperature and snow depth bias correction is in the "good" category, and precipitation is in the "fair" category.

Table 3. Validation of used ESM model using the Normalized Root Means Square Error (NRMSE) of the bias corrected historical (1985-2014) model data against ERA5-land.

Variables	**T max**	**T min**	**Precipitation**	**Snow depth**
Model	Tays	MRI-ESM2.0	NorESM2-MM	MRI-ESM2.0
NRMSE (%)	8.7	11.5	23.7	15.4
Accuracy	Excellent	Good	Fair	Good

3.2 Observed drought.

Figure 3 shows the seasonal (including January-March, April-June, July-September, and October-December) and annual time series of observed drought indicators during 1985-2014. The figure's upper, middle, and lower panel figures represent SMRI, SPEI, and SPI, respectively. Their annual trend is also drawn on each of the graphs. Details of seasonal and annual time trends are shown in Table 4. From Figure 3 and Table 3, the stronger decreasing trend of snow- and precipitation-evapotranspiration-based drought indices of SMRI (Fig. 3, top) and SPEI (Fig., middle) are apparent compared to the precipitation-only dependent drought index of SPI (Fig., bottom). The annual trend of SPI drought is almost zero, which shows that the decrease in precipitation in the last two decades was not significant at a 5% level and is within the range of normal fluctuation. However, the annual trend of SMRI and SPEI drought index is -0.068 and -0.079, respectively, which is significant at the 5% level. Figure 3 presents two significant issues regarding the annual and seasonal future changes of drought types. Firstly, on an annual scale, the SMRI and SPEI, which are temperature-based drought indices, show an increasing drought trend until the end of the century.

In contrast, the precipitation-based drought index SPI does not exhibit significant changes in the basin's drought. This situation indicates that the negative water balance drought in the basin is primarily due to increased evapotranspiration caused by rising temperatures rather than a decrease in precipitation. Secondly, on a seasonal scale, the trend of changes in the temperature-based drought indices of SMRI and SPEI is almost similar in different seasons. In contrast, the precipitation-based drought index of SPI shows less similarity in the drought trend across different seasons. This demonstrates that the impact of rising temperature on the basin's drought is much more significant and carries more weight than precipitation.

https://doi.org/10.5194/hess-2024-48
Preprint. Discussion started: 26 February 2024

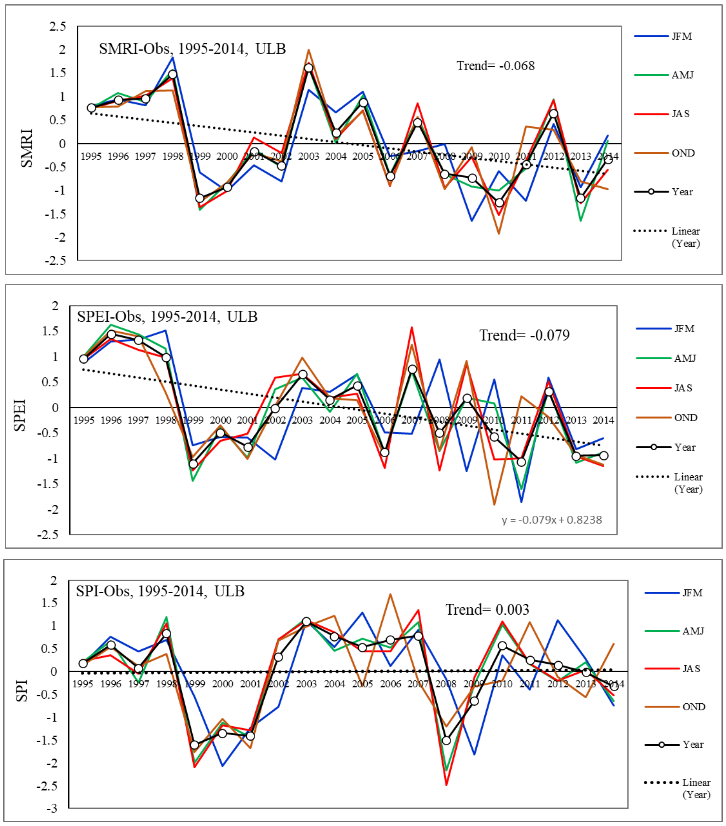

Figure. 3. Seasonal to yearly SMRI (upper), SPEI (middle) and SPI (lower) drought indices (bold lines) accompanied by yearly trend line (dashed) based on ERA5-land data during 1995-2014.

3.3 Future drought characteristics

Drought characteristics over ULB by using SMRI, SPEI, and SPI in the near (2021-2040), mid (2041-2060), and far (2081-2100) future periods under SSP1-2.6, SSP2-4.5, and SSP5-8.5 have been projected using bias-corrected precipitation and temperature data retrieved from the seven CMIP6 models described in table 1.

https://doi.org/10.5194/hess-2024-48
Preprint. Discussion started: 26 February 2024

3.3.1 Drought Frequency

As shown in Figure 4, the mean SMRI drought frequency over ULB has an increasing trend from the near future to the far future, as well as from SSP1-2.6 to SSP5-8.5, with the highest increase in SSP5-8.5. Shortly (2021-2040) under the SSP1-2.6 scenario, the high-frequency droughts with a frequency between 16 and 20 times per 20-year are mostly limited over the southern part of the Lake, while in mid (2041-2060) and far (2081-2100) future period, the area has been expanded to the all-eastern part of the Lake as well as eastern and southern lowlands of the basin. In the future, the high-frequency drought will spread to the foothill areas further from the east of the Lake, showing a decrease in snowmelt runoff on the high Sahand mountain range. The low frequency of SMRI droughts, with less than four events per 20 years, is assigned to the western and southern regions of the basin in the SSP1-2.6 scenario. Under the SSP2-4.5 scenario, the drought-affected area with a high frequency of events in the near future is almost twice that of SSP1-2.6. Drought with the frequency of 10-12 times per 20-year will emerge over most of the northeastern part of the basin in the future.

Interestingly, under the SSP5-8.5 scenario, the drought-affected area of high frequency in the near future is like SSP2-4.5, except for the most northeastern part of the basin (which is expected to experience drought frequency of 4-6 times per 20-year). What is essential in this scenario is that the affected area of high-frequency (more than sixteen times per 20-year) droughts are almost unchanged, but the affected area of moderate frequency (8-12 times per 20-year) droughts has increased significantly. According to the SMRI, the drought in the high mountain areas decreases less than in the low land areas and the foothills. This may be because the increase in temperature in lowlands and foothills areas causes a decrease in snowfall, which results in a decrease in runoff.

https://doi.org/10.5194/hess-2024-48
Preprint. Discussion started: 26 February 2024

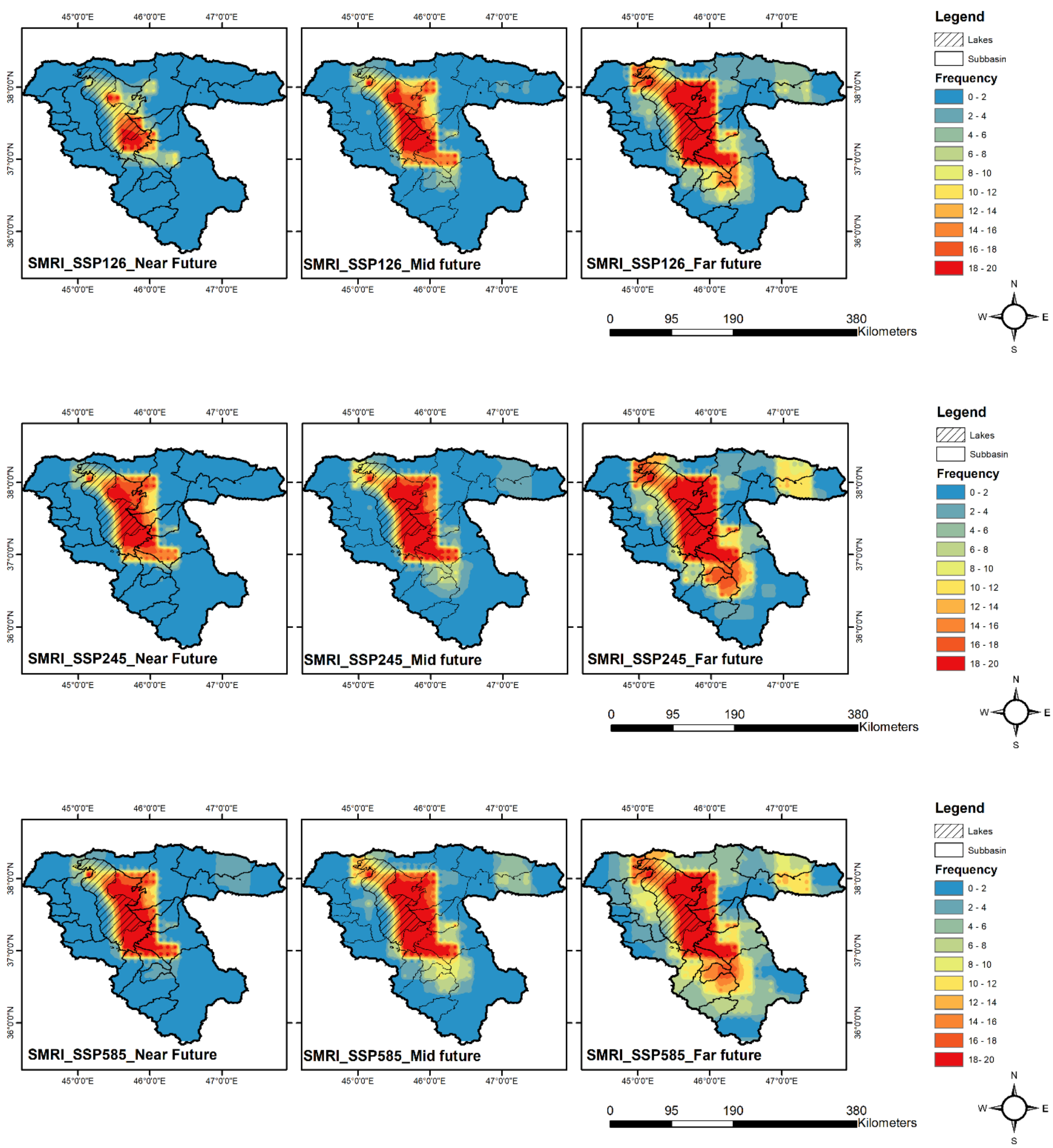

Figure 4. Maps showing SMRI drought frequency over ULB in the near (2021-2040), mid (2041-2060), and far (2081-2100) future under SSP1-2.6, SSP2-4.5, and SSP5-8.5

https://doi.org/10.5194/hess-2024-48
Preprint. Discussion started: 26 February 2024

Hydrology and Earth System Sciences
Open Access
Discussions

The future of drought-affected areas using SPEI (thus excluding the role of snow) for ULB is shown in supplementary figure S1 (in supplementary section). Contrary to SMRI droughts, the area-averaged frequency of SPEI droughts in the ULB is projected to extend and cover most of the basin's area under all three emissions scenarios. SPEI drought in the future is more extensive and widespread than SMRI (Figure 4) and SPI (not shown). This is undoubtedly due to the direct effect of the rising temperature, which increases potential evapotranspiration. Under SSP1-2.6, the regions at the western, eastern, and near-southern boundaries of the ULB are expected to experience the lowest drought frequency of less than four events per 20 years in the near future. The frequency will increase in the mid and far future, especially over the Lake and the southern part of ULB. The maximum drought frequency is concentrated over the Lake, colored in red, which indicates 18-20 drought events per 20 years. The most frequent drought events are projected to occur under SSP5-8.5, showing that almost all areas of ULB will experience at least one drought every two years, while the Lake and its eastern part will face a drought yearly. While the frequency of droughts in the SSP1-2.6 and SSP5-8.5 scenarios increases from the near to the far future, the increase in the SSP2-4.5 scenario is less. The different pictures of SMRI and SPEI's drought-affected areas point to snow cover's role in impacting drought events. Unlike SMRI and SPEI, the frequency of SPI drought (not shown) does not show an apparent increase under different scenarios and periods. This may be because it is not directly a function of temperature as well as runoff. However, it shows a slight increasing trend under the SSP5-8.5 scenario. All diverse types of drought indices show that the mountainous areas of the basin will experience the most minor drought. In contrast, most droughts occur in the basin's lowland (including lakes) and foothill areas.

3.3.2 Drought Severity

Figure 5 shows the future projection of SMRI drought severity spatial patterns over ULB. Drought severity will increase from the near to the far future, but the increase in SSP5-8.5 is

https://doi.org/10.5194/hess-2024-48
Preprint. Discussion started: 26 February 2024

more significant than in the other two scenarios. The drought severity in SSP2-4.5 is only slightly greater than that of SSP1-2.6. Besides the more robust projected temperature increase of the SSP5-8.5 scenario for ULB, it will also force the westerlies and their accompanying precipitation weather systems to move northward (Rasuli et al., 2012), meaning they receive less precipitation. In the near future, the magnitude of accumulated drought severity is 9 to 12 units over the Lake under the SSP1-2.6 scenario, 12 to 15 units under the SSP2-4.5 scenario, and 15 to 18 units under the SSP5-8.5 scenario. In the far future, the drought severity is projected to be 15-20, 18-20, and 20-22 units under the SSP1-2.6, SSP2-4.5, and SSP5-8.5 scenarios, respectively. It is essential to notice that the severity is projected to be most pronounced in the central parts of the basin, which are the areas already experiencing prominent levels of aridity today and are, therefore, particularly vulnerable to drying. The drying severity is also projected to increase in the Lake. This is because the lakes rely on snowmelt for their water supply, and the drying is projected to reduce the amount of available snowmelt.

https://doi.org/10.5194/hess-2024-48
Preprint. Discussion started: 26 February 2024

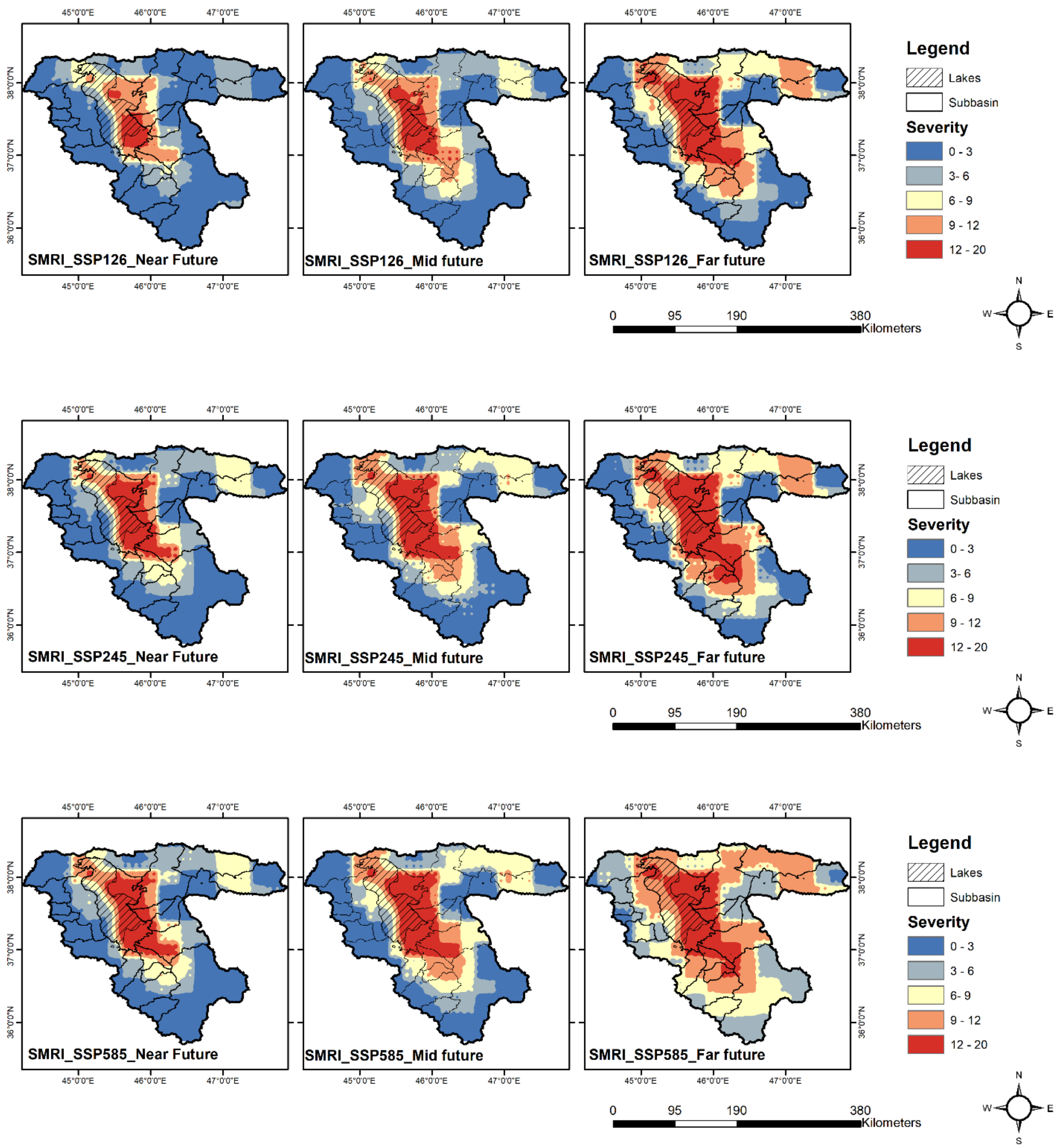

Figure 5. Maps showing SMRI drought severity over ULB in the near (2021-2040), mid (2041-2060), and far (2081-2100) future under SSP1-2.6, SSP2-4.5, and SSP5-8.5

https://doi.org/10.5194/hess-2024-48
Preprint. Discussion started: 26 February 2024

Hydrology and Earth System Sciences
Open Access
Discussions

The severity of droughts characterized by SPEI is projected to increase (by both values and affected area) under all SSP forcing scenarios (Figure S2 in supplementary material section). The maps also show that the west-central parts of the basin are projected to experience the most severe drought conditions, the western and southern parts of the basin are projected to experience mild to moderate drought conditions in the near future and moderate to severe drought conditions in the middle future. The central and eastern parts of the basin are projected to experience moderate to severe drought conditions in the near future and severe to extreme drought conditions in the middle and far future. In the case of SPI (figure S3, in supplementary section), the extent of drought-affected areas is less than SPEI and SMRI, which shows that temperature and snow melt are among the factors of drought extent in these regions. Unlike the SPEI and SMRI, the precipitation deficit forced droughts, as described by the SPI (for both severity and affected area), do not show an increasing trend over time. The western half and some areas in the southern parts of the basin are projected to be most affected by precipitation deficit droughts. Interestingly, the severity and affected area of precipitation deficit droughts will generally decrease in ULB for both the mid and near future under SSP scenarios 1-2.6 and 5-8.5. Only scenario SSP 2-4.5 shows both an increase in severity and an affected area of SPI droughts. The SPI is projected to become even more severe in the mid-future (2041-2060) and affect more areas toward the western and southern parts of the basin. The central and eastern parts of the basin are projected to experience severe to extreme drought conditions. The SPI is projected to become the most widespread in the far future (2081-2100. The central and eastern parts of the basin are projected to experience extreme to exceptional drought conditions.

3.4 Analysis of uncertainty

Temporal evolutions of basin-scale drought are shown in Figure 6 for SPI, SPEI, and SMRI drought indices under SSP1-2.6, SSP2-4.5, and SSP5-8.5 scenarios. The observed drought

https://doi.org/10.5194/hess-2024-48
Preprint. Discussion started: 26 February 2024

Hydrology and Earth System Sciences
Discussions

indices in 1985-2014 are shown in black dashed lines, while the projected drought indices are shown in colored dashed lines. The shaded areas around the colored dash lines represent the future projection uncertainty among emission scenarios, which covers the range of the upper 75th percentile and the lower 25th percentile of projections in the annual time scale. However, the decline in drought indices is more pronounced under the high-emission SSP5-8.5 scenarios. A basin-scale drought hiatus in the 2080s and later can be seen both in SMRI and SPEI indices under SSP1-2.6, which may be due to the reduction of greenhouse gas emissions in this scenario at the end of the 21st century. Such a hiatus in SMRI and SPEI drought indices can be seen around the 2090s under the SSP2-4.5 scenario. The SPI graph shows that future SPI uncertainty is more significant under the high-emission scenario.

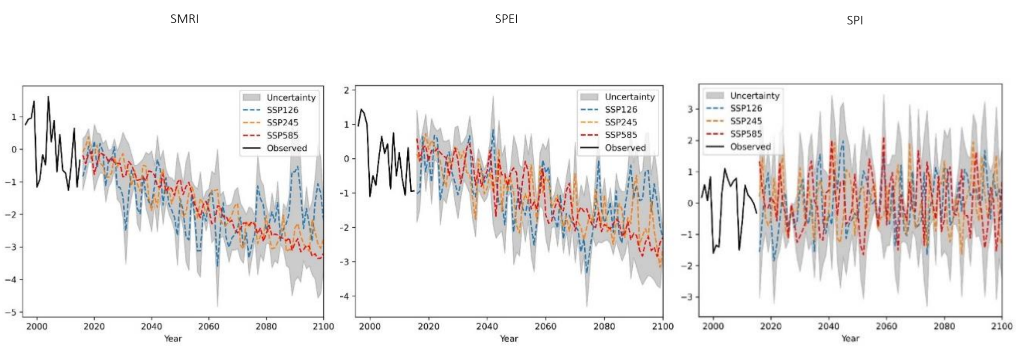

Figure 6. Future drought projection over the ULB based on SPI, SPEI and SMRI based on SSP1-2.6, SSP2-4.5 and SSP5-8.5 scenarios, with related uncertainties.

Under the SSP1-2.6 scenario for the near future (2021-2040), 79% of the basin is projected to experience drought using SPI, with the SPEI and SMRI index indicating 96% and 72%, respectively. The scenario's mid-future projections (2041-2060) suggest a decrease in SPI-affected regions to 74%, with the SPEI remaining comparably high at 95% and an increase in SMRI to 83%. By the far future (2081-2100', the basin's SPI-projected drought area diminishes to 48%, the SPEI drops to 86%, and the SMRI rises to 87%. Shifting the focus to the SSP2-4.5

https://doi.org/10.5194/hess-2024-48
Preprint. Discussion started: 26 February 2024

Hydrology and Earth System Sciences
Open Access
EGU
Discussions

scenario, the near-future data projects that 73% of the basin will be under SPI-defined drought, 94% under SPEI, and 65% using the SMRI index. The mid-future timeframe indicates a rise in SPI to 58%, a slight decrease in SPEI to 92%, and an increase in SMRI to 77%. For the future, the SPI jumps to 79%, and the SPEI and SMRI suggest intensified drought conditions at 94% and 84%, respectively. Finally, under the SSP5-8.5 pathway, the near-future period experienced 59% of the basin affected by SPI drought, 92% by SPEI, and 64% by SMRI. The mid-future period marks an increase in SPI to 76%, SPEI to 93%, and SMRI remaining consistent at 76%. In the far future, the SPI will extend to cover 80% of the basin, the SPEI will rise further to 96%, and the SMRI indicates a significant increase to 99% (Figure 7).

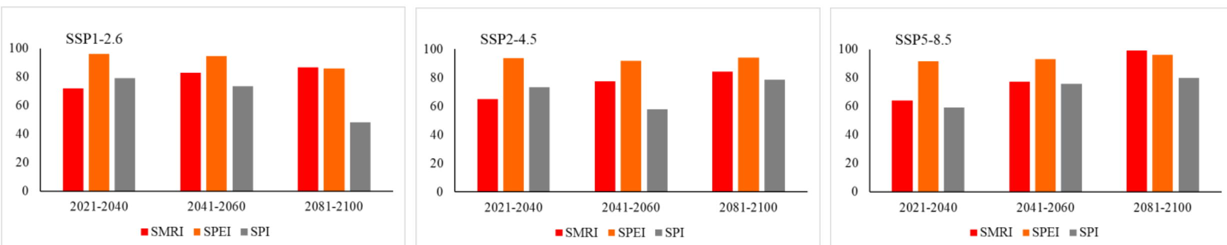

Figure 7. Drought affected areas in the ULB under different scenarios SSP1-2.6(left), SSP2-4.5(center) and SSP5-8.5(right) for 2021-40, 2041-60 and 2081-2100, respectively.

The decadal evolution of drought-affected areas, accompanied by their uncertainty, is shown in Figure 8. Two precise results can be derived from the basin-wide temporal evolution of droughts in the ULB. The first one is that the drought-affected area described by the SPI does not show a clear trend, while the increasing trend of drought-affected areas described by the SMRI is obvious. By summing up the different classes of drought, the relative drought-affected area of the basin was calculated for near, mid, and far future decades. Our results show no significant changes in the drought-affected area in the future compared to today's drought area (the observation period) both in SPI and SPEI indices. The low future trend of SPEI drought-affected areas may be due to the lack of sufficient moisture to evaporate in more warming conditions. However, in the case of SMRI, drought-affected areas will increase

https://doi.org/10.5194/hess-2024-48
Preprint. Discussion started: 26 February 2024

Hydrology and Earth System Sciences
Discussions

significantly from about 20% in the recent future (2021-2040) to 60% in the far future period of 2081-2100.

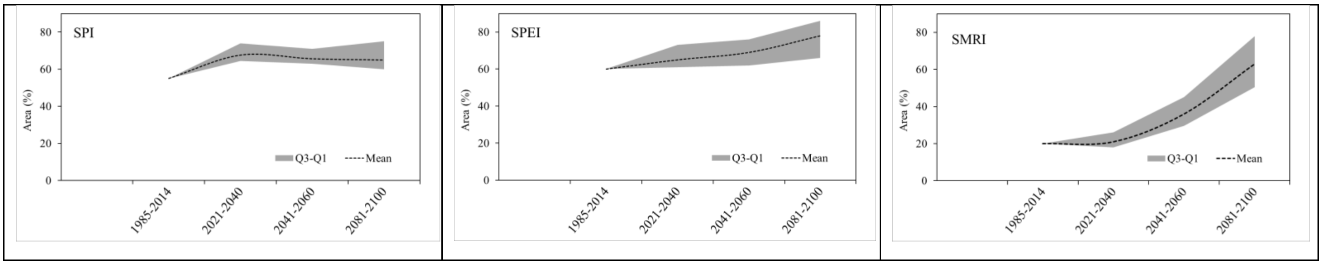

Figure 8. Basin-wide future decadal evolution of drought affected area for ULB described by the SPI, SPEI and SMRI with their uncertainties of the 25 and 75 quantiles of the used ensemble of SSP scenarios.

3.5 Drought characteristic

The future characteristics of SPI, SPEI and SMRI drought including Severity, Frequency and Duration have been shown in a three-dimensional plot in Figure 9 over ULB under SSP1-2.6, SSP2-4.5 and SSP5-8.5 in near future (2021-2014), middle future (2041-2060) and far future (2081-2100). The threshold value of -1 was used to represent a drought condition. The SPI, SPEI, and SMRI all show increased drought severity, frequency, and duration under all three SSP scenarios. The severity, frequency and duration of droughts is projected to increase the most under SSP5-8.5, followed by SSP2-4.5 and SSP1-2.6 Among all drought indicators, the SPI drought index does not show clear changes in future periods and scenarios. This shows that in the future, despite the decrease in rainfall in the Urmia Basin, it will be within its natural fluctuations. The three-dimensional diagram of the future droughts of the basin clearly shows the intensification of droughts in the ULB based on SMRI and SPEI indicators in the mid

https://doi.org/10.5194/hess-2024-48
Preprint. Discussion started: 26 February 2024

Hydrology and Earth System Sciences
Open Access
Discussions

and far future periods specifically for SMRI drought index, showing strong decrease in runoff of the basin.

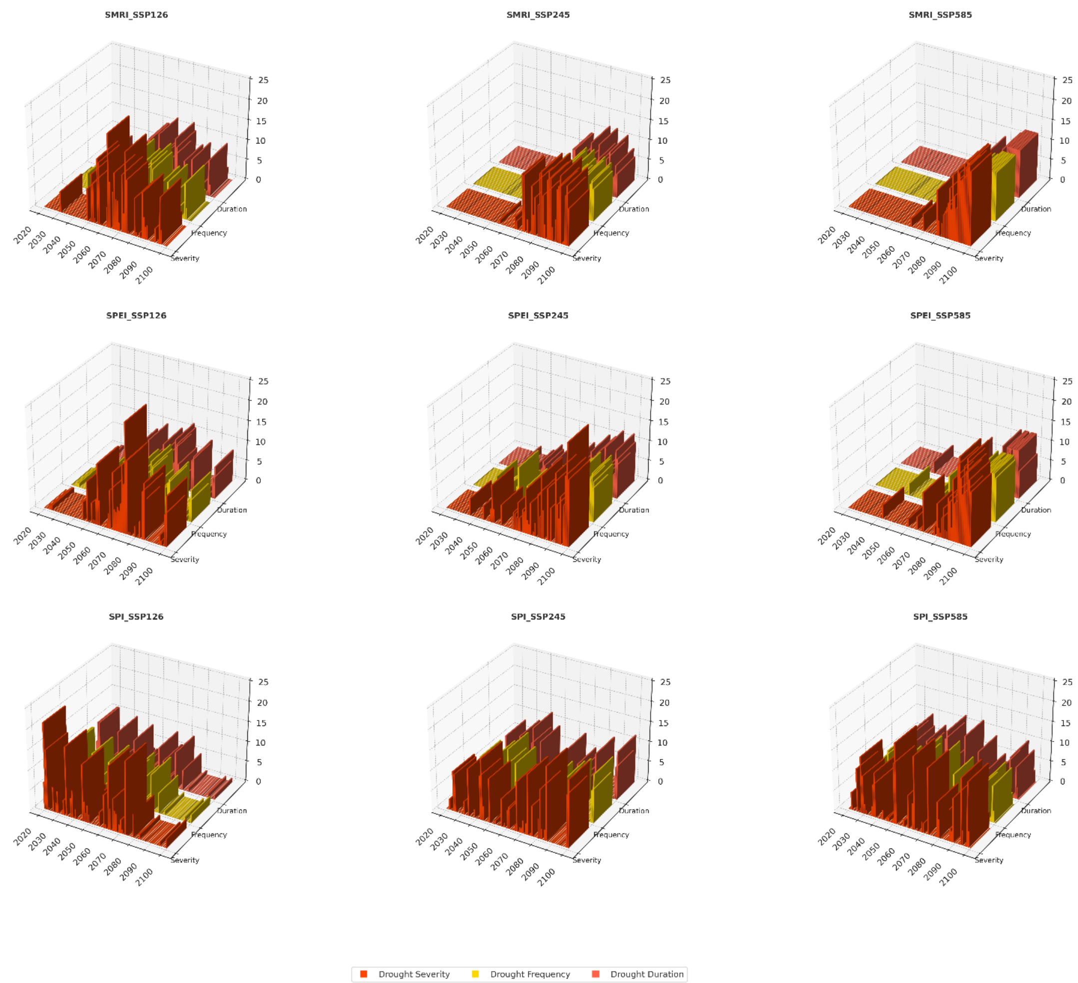

Figure 9. Three-dimensional representation of future drought projection over ULB under SSP1-2.6, SSP2-4.5 and SSP5-8.5 in near future (2021-2014), middle future (2041-2060) and far future (2081-2100)

4 Conclusion

This study investigates the implications of bias corrected hydrometeorological variables of selected CMIP6 on the future projection of precipitation-, evapotranspiration- and

https://doi.org/10.5194/hess-2024-48
Preprint. Discussion started: 26 February 2024

snowmelt-based drought indicators of SPI, SPEI and SMRI over Urmia Lake Basin (ULB) located in the northwest of Iran. The basin is in the neighborhood of Türkiye, Azerbaijan, and Armenia from west and north. A thorough analysis of drought indices in the observation period and future period was performed to project future drought of the basin. Three scenarios of SSP1-2.6, SSP2-4.5 and SSP5-8.5 were utilized to provide a comprehensive understanding of the potential impacts of climate change on future drought of the basin. By considering SSP scenarios, this study offers valuable insights into the past and future drought conditions to address the future drought characteristics posed by climate change over the basin. In this study, some key findings have been identified to summarize the results. First, the accuracy varies across different climate variables when assessing model performance using the NRMSE metric. The bias correction method exhibits excellent skill in simulation maximum temperature (TaiESM), well for minimum temperature (MRI-ESM2.0), fair for precipitation (NorESM2-MM), and maintains good performance for snow (MRI-ESM2.0).

Based on observed drought trends, the decreasing trend has been found in SMRI and SPEI indices, while there was no significant trend in SPI. The annual trend of SPI drought appears stagnant, indicating that the reduction in precipitation over the last two decades falls within the normal fluctuation. In contrast, the annual trend of SMRI and SPEI drought indices demonstrates statistical significance at the 5% level.

Examining future SMRI drought projections reveals an increasing trend over ULB from the near to the far future, especially under the SSP5-8.5 scenario. This trend extends further into the foothill areas east of the lake, reflecting decreased snowmelt runoff from the high Sahand mountain range. Interestingly, the high mountain areas experience a smaller decrease in drought than lowland and foothill areas, due to temperature-driven reductions in snowfall and runoff. Future SMRI and SPEI drought projections indicate a more extensive and widespread drought scenario compared to SPI, with a higher amount of future trend in SMRI drought index. This heightened drought occurrence is attributed to rising temperatures' direct impact on increasing evapotranspiration and runoff, with

https://doi.org/10.5194/hess-2024-48
Preprint. Discussion started: 26 February 2024

the most frequent drought events anticipated under SSP5-8.5. The drought frequency map for the far future under SSP5-8.5 predicts drought occurrences throughout ULB, with annual droughts affecting the lake and its eastern regions. In contrast to SMRI and SPEI, future SPI drought projections exhibit a less distinct increase across various scenarios and periods, likely because SPI is not directly influenced by temperature or runoff. Nevertheless, a slight increasing trend is observed under the SSP5-8.5 scenario.

Finally, when considering scenario and drought indices uncertainty, our study indicates that SMRI exhibits lower uncertainty than SPEI and SPI, offering a high level of certainty regarding the exacerbation of runoff drought. However, in the far future, the uncertainty of SMRI increases. The uncertainty associated with the other two indices remains relatively low, with the SPEI drought index displaying a modest increasing trend, albeit lower than SMRI. Notably, the decline in drought indices becomes more pronounced under the high-emission scenario of SSP5-8.5. These findings collectively provide valuable insights into the complex dynamics of drought in the ULB region, offering critical information for future climate adaptation and water resource management strategies. The SPI, SPEI, and SMRI all show increased drought severity, frequency, and duration under all three SSP scenarios. The severity, frequency and duration of droughts is projected to increase the most under SSP5-8.5, followed by SSP2-4.5 and SSP1-2.6. Among all drought indicators used, the SPI drought index does not show clear changes in future periods and scenarios. This shows that in the future, despite the decrease in precipitation in the Urmia Basin, it will be within its natural fluctuations. The three-dimensional diagram of the future droughts of the basin shows the intensification of droughts in the ULB based on SMII and SPEI indicators in the mid and far future periods specifically for SMRI drought index, showing strong decrease in runoff of the basin. As the end of century, a basin scale drought hiatus in the 2080s and later can be seen both in SMRI and SPEI indices under SSP1-2.6, which may be due to the reduction of greenhouse gas emissions in this scenario at the end of 21st century under Paris climate agreement. Such hiatus in SMRI and SPEI drought indices can be seen around 2090s

https://doi.org/10.5194/hess-2024-48
Preprint. Discussion started: 26 February 2024

under SSP2-4.5 scenario. Intensification of SMRI drought in the basin is consistent with study of the Saboor and Mirmousavi (2014) and Habibi et al. (2021) which found an annual decrease in snowfall trend around ULB during observation period. A dropped in snow melt water supply over Asia was confirmed by Kraaijenbrink (2021). IPCC AR6 has also projected changes in the annual mean runoff in selected river basins of the earth at global warming levels of 1.5°C, 2°C and 4°C in a combined ensemble. In this study, runoff decrease in Euphrates and Helmand (the basins closest to ULB), projected to be 72-78% and 65-69%, respectively (IPCC, 2022).

Author Contributions

All authors contributed to the study’s conception and design. M.H. undertook data preparation and processing and provided all maps. She also wrote the first draft of the manuscript. W.S. supervised the project and was the original source for the main idea. He also had a significant role in editing, reviewing, and finalizing the results. I.B. finalized the draft text and performed editing and reviewing. He was also active in gathering and reviewing data and was responsible for the statistical calculations. All authors have read and agreed to the published version of the manuscript.

Competing interests

The authors declare that they have no conflict of interest.

References

Abbasi, F.; Kohi, M.; Flamarzi, Y.; Javanshri, Z.; Malbousi, S.; Babaeian, I.: *Investigation and analysis of Iran's annual temperature and precipitation trend (2017-1988)*, Nivar, 43(106-107), 10.30467/NIVAR.2019.184059.1128, (2019).

Adnan, M.; Nabi, Gh.; Poomee, M. S.; Ashraf, A.: *Snowmelt runoff prediction under changing climate in the Himalayan cryosphere: A case of Gilgit River Basin*, Geoscience Frontiers, 8(5), 941-949, https://doi.org/10.1016/j.gsf.2016.08.008, (2017).

https://doi.org/10.5194/hess-2024-48
Preprint. Discussion started: 26 February 2024

Ali, M.; Asad, F.; Zhu, H.; Ahmed, M.; Sigdel, S. R. H.; Ru, S. S. L.; Eryun, H. I.; Yaseen, T.: *Dendrochronological Investigation of selected Conifers from Karakoram-Himalaya. Northern Pakistan*, Pak J Bot, 53:3, 10.30848/PJB2021-3(20), (2019).

Alizadeh-Choobari, O.; Ahmadi-Givi, F.; Mirzaei, N.; Owlad, E.: *Climate change and anthropogenic impacts on the rapid shrinkage of Lake Urmia*, Int. J. Climatol., 36, 4276–4286, https://doi.org/10.1002/joc.4630, (2016).

An, S.; Park, G.; Jung, H.; Jang, D.: *Assessment of Future Drought Index Using SSP Scenario in Rep. of Korea*, Sustainability, 14, 4252, https://doi.org/10.3390/su14074252, (2022).

Andreadis, K. M.; Clark, E. A.; Wood, A. W.; Hamlet, A. F.; Lettenmaier, D. P.: *Twentieth-century drought in the conterminous United States*, J. Hydrometeorol., 6, 985–1001, https://doi.org/10.1175/JHM450.1, (2005).

Bazaz, A.; Bertoldi, P.; Buckeridge, M.; Cartwright, A.; de Coninck, H.; Engelbrecht, F.; Jacob, D.; Hourcade, J.-C.; Klaus, I.; de Kleijne, K.; Lwasa, S.; Markgraf, C.; Newman, P.; Revi, A.; Rogelj, J.; Schultz, S.; Shindell, D.; Singh, C.; Iecki, W.; Waisman, H.: *Summary for urban policymakers: What the IPCC Special Report on global warming of 1.5°C means for cities*, IHHS Indian Institute for Human Settlements, Bengaluru. India, https://doi.org/10.24943/SCPM.2018, (2018).

Bergstrom, S.; Harlin, J.; Lindström, G.: *Spillway design floods in Sweden: I. New guidelines*, Hydrol. Sci. J., 37(5), 505–519, 10.1080/02626669209492615, (1992).

Bock, L.; Lauer, A.; Schlund, M.; Barreiro, M.; Bellouin, N.; Jones, C.; Meehl, G. A.; Predoi, V.; Roberts, M. J.; Eyring, V.: *Quantifying progress across different CMIP phases with the ESMValTool*, J. Geophys. Res. Atmos., 125: e2019JD032321, https://doi.org/10.1029/2019JD032321, (2020).

Chen, H.; Sun, J.; Lin, W.; Xu, H.: *Comparison of CMIP6 and CMIP5 models in simulating climate extremes*, Sci. Bull., 65: 1415–1418, 10.1016/j.scib.2020.05.015, (2020).

Cowherd, M.; Leung, L. R.; Girotto, M.: *Evolution of global snow droughts characteristics from 1850 to 2100*, Environmental Research Letters, 10.1088/1748-9326/acd804, (2023).

EC-Earth Consortium (EC-Earth): *EC-Earth-Consortium EC-Earth3 model output prepared for CMIP6 CMIP historical*, Version 20230617.Earth System Grid Federation, https://doi.org/10.22033/ESGF/CMIP6.4700, (2019).

Ghajarnia, N.; Akbari, M.; Saemian, P.; Ehsani, M. R.; Hosseini-Moghari, S.-M.; Azizian, A.; et al.: *Evaluating the evolution of ECMWF precipitation products using observational data for Iran: From ERA40 to ERA5*, Earth and Space Science, 9, e2022EA002352, https://doi.org/10.1029/2022EA002352, (2022).

Huning, L. S.; AghaKouchak, A.: *Global snow drought hot spots and characteristics*, P. Natl. Acad. Sci. USA, 117, 19753–19759, https://doi.org/10.1073/pnas.1915921117, (2020).

Huning, L. S.; AghaKouchak, A.: *Global snow drought hot spots and characteristics*, Proc Natl Acad Sci U S A, 117(33):19753-19759, doi: 10.1073/pnas.1915921117, (2020).

Huo-Po, C.; Jian-Qi, S.; Xiao-Li, C.: *Future changes of drought and flood events in China under a global warming scenario*, Atmos Oceanic Sci Lett, 6:8–13, 10.1080/16742834.2013.11447051, (2013).

Huss, M.; Bookhagen, B.; Huggel, C.; Jacobsen, D.; Bradley, R.S.; Clague, J.J.; Vuille, M.; Buytaert, W.; Cayan, D.R.; Greenwood, G.; Mark, B.G.; Milner, A.M.; Weingartner, R.; Winder, M.: *Toward mountains without permanent snow and ice*, Earth's Future, 5, 418-435, https://doi.org/10.1002/2016EF000514, (2017).

IPCC, 2022: *Climate Change 2022: Impacts, Adaptation, and Vulnerability. Contribution of Working Group II to the Sixth Assessment Report of the Intergovernmental Panel on Climate Change*, [H.-O. Pörtner, D.C. Roberts, M. Tignor, E.S. Poloczanska, K. Mintenbeck, A. Alegría, M. Craig, S. Langsdorf, S. Löschke, V. Möller, A. Okem, B. Rama (eds.)], Cambridge University Press, Cambridge, UK and New York, NY, USA, 3056 pp., 10.1017/9781009325844, (2022).

IPCC: *Climate Change 2021: The Physical Science Basis. Contribution of Working Group I to the Sixth Assessment Report of the Intergovernmental Panel on Climate Change*, Cambridge, UK: Cambridge University Press, https://doi.org/10.1017/9781009157896.005, (2021).

Izadi, N.; Karakani, E. G.; Saadatabadi, A. R.; Shamsipour, A.; Fattahi, E.; Habibi, M.: *Evaluation of ERA5 Precipitation Accuracy Based on Various Time Scales over Iran during 2000–2018*, Water, 13(18):2538, https://doi.org/10.3390/w13182538, (2021).

https://doi.org/10.5194/hess-2024-48
Preprint. Discussion started: 26 February 2024

Hydrology and Earth System Sciences Discussions
Open Access
EGU

Izadi, N.; Karakani, E. G.; Saadatabadi, A. R.; Shamsipour, A.; Fattahi, E.; Habibi, M.: *Evaluation of ERA5 Precipitation Accuracy Based on Various Time Scales over Iran during 2000–2018*, Water, 13(18):2538, https://doi.org/10.3390/w13182538, (2021).

Khaniani, A. S.; Mohammadi, A.: *Comparison of ERA5-Land reanalysis data with surface observations over Iran*, Iranian Journal of Geophysics, 16(1), 195-212, 10.30499/ijg.2022.313494.1376, (2022).

Kim, J.-B.; So, J.-M.; Bae, D.-H.: *Global warming impacts on severe drought characteristics in Asia monsoon region*, Water, 12:1360, https://doi.org/10.3390/w12051360, (2020).

Kraaijenbrink, P.D.A.; Stigter, E.E.; Yao, T. et al.: *Climate change is decisive for Asia's snow meltwater supply*, Nat. Clim. Chang., 11, 591–597, https://doi.org/10.1038, (2021).

Lee, Wei-Liang; Liang, Hsin-Chien: *AS-RCEC TaiESM1.0 model output prepared for CMIP6 CMIP historical*, Version 20230617.Earth System Grid Federation, https://doi.org/10.22033/ESGF/CMIP6.9755, (2020).

Lovato, T.; Peano, D.; Butenschön, M.; Materia, S.; Iovino, D.; Scoccimarro, E. et al.: *CMIP6 simulations with the CMCC Earth System Model (CMCC-ESM2)*, Journal of Advances in Modeling Earth Systems, 14, e2021MS002814, https://doi.org/10.1029/2021MS002814, (2022).

Malayeri, A. K.; Saghafian, B.; Raziei, T.: *Performance evaluation of ERA5 precipitation estimates across Iran*, Arab J Geosci, 14, 2676, https://doi.org/10.1007/s12517-021-09079-8, (2021).

Mokhtari, R.; Akhoondzadeh, M.: *Data Fusion and Machine Learning Algorithms for Drought Forecasting Using Satellite Data*, Journal of the Earth, and Space Physics, 46(4), 231-246, 10.22059/jesphys.2020.299445.1007199, (2021).

Mondal, S.; Mishra, K. A.; Leung, R. et al.: *Global droughts are connected by linkages between drought hubs*, Nat Commun, 14, 144, https://doi.org/10.1038/s41467-022-35531-8, (2023).

Muñoz-Sabater, J.; Dutra, E.; Agustí-Panareda, A.; Albergel, C.; Arduini, G.; Balsamo, G.; Boussetta, S.; Choulga, M.; Harrigan, S.; Hersbach, H.; Martens, B.; Miralles, D. G.; Piles, M.; Rodríguez-Fernández, N. J.; Zsoter, E.; Buontempo, C.; Thépaut, J.-N.: *ERA5-Land: a state-of-*

https://doi.org/10.5194/hess-2024-48
Preprint. Discussion started: 26 February 2024

the-art global reanalysis dataset for land applications, Earth Syst. Sci. Data, 13, 4349–4383, https://doi.org/10.5194/essd-13-4349-2021, (2021).

Myers, D. T.; Ficklin, D. L.; Robeson, S. M.: *Hydrologic implications of projected changes in rain-on-snow melt for Great Lakes Basin watersheds*, Hydrol. Earth Syst. Sci., 27, 1755–1770, https://doi.org/10.5194/hess-27-1755-2023, (2023).

Parajka, J.; Blaschke, A. P.; Blöschl, G.; Haslinger, K.; Hepp, G.; Laaha, G.; Schöner, W.; Trautvetter, H.; Viglione, A.; Zessner, M.: *Uncertainty contributions to low-flow projections in Austria*, Hydrol. Earth Syst. Sci., 20, 2085–2101, https://doi.org/10.5194/hess-20-2085-2016, (2016).

Rasuli, A. A.; Babaeian, I.; Ghaemi, H.; Zawar-reza, P.: *Analysis the time series of the central pressure of synoptic weather system affecting seasonal precipitation of Iran*, Geography and Development, 10(27), 77-88, 10.22111/gdij.2012.486, (2012).

Saavedra, F. A.; Kampf, S. K.; Fassnacht, S. R.; Sibold, J. S.: *Changes in Andes snow cover from MODIS data, 2000–2016*, The Cryosphere, 12, 1027–1046, https://doi.org/10.5194/tc-12-1027-2018, (2018).

Saboor, L.; Mirmousavi, S.: *Study of snow precipitation changes trend in North West of Iran*, Geography and Environmental Planning, 25(3), 119-136, 20.1001.1.20085362.1393.25.3.10.6, (2014).

Shafer, B.; Dezman, L.: *Development of a surface water supply index (SWSI) to assess the severity of drought conditions in snowpack runoff areas*, Proceedings of the Western Snow Conference, vol. 50, pp. 164–175, Western Snow Conference, Reno, Nev., sites/westernsnowconference.org/PDFs/1982Shafer.pdf (1982).

Sharma, S.; Hamal, K.; Khadka, N.; Ali, M.; Subedi, M.; Hussain, G.; Ehsan, M. A.; Saeed, S.; Dawadi, B.: *Projected Drought Conditions over Southern Slope of the Central Himalaya Using CMIP6 Models*, Earth System and Environment, 5, 849–859, https://doi.org/10.1007/s41748-021-00254-1, (2021).

Sheffield, J.; Wood, E. F.; Roderick, M. L.: *Little change in global drought over the past 60 years*, Nature, 491, 435–438, https://doi.org/10.1038/nature11575, (2012).

Staudinger, M.; Stahl, K.; Seibert, J.: *A drought index accounting for snow*, Water Resour. Res., 50, 7861–7872, 10.1002/2013WR015143, (2014).

Supharatid, S.; Nafung, J.: *Projected drought conditions by CMIP6 multimodel ensemble over Southeast Asia*, Journal of Water and Climate Change, 12(7), 3330–3354, doi: https://doi.org/10.2166/wcc.2021.308, (2021).

Tahir, A. A.; Chevallier, P.; Arnaud, Y.; Neppel, L.; Ahmad, B.: *Modeling snowmelt-runoff under climate scenarios in the Hunza River basin, Karakoram Range, Northern Pakistan*, Journal of Hydrology, 409(1–2), 104-117, https://doi.org/10.1016/j.jhydrol.2011.08.035, (2011).

Taylor, K. E.: *Summarizing multiple aspects of model performance in a single diagram*, J. Geophys. Res., 106, 7183–7192, 10.1029/2000JD900719, (2001).

Tijdeman, E.; Barker, L. J.; Svoboda, M. D.; Stahl, K.: *Natural and human influences on the link between meteorological and hydrological drought indices for a large set of catchments in the contiguous United States*, Water Resources Research, 54, 6005–6023, https://doi.org/10.1029/2017WR022412, (2018).

Van Loon, A. F.; Ploum, S. W.; Parajka, J.; Fleig, A. K.; Garnier, E.; Laaha, G.; Van Lanen, H. A. J.: *Hydrological drought types in cold climates: Quantitative analysis of causing factors and qualitative survey of impacts*, Hydrology and Earth System Sciences, 19(4), 1993–2016, http://doi.org/10.5194/hess-19-1993-2015, (2015).

Vicente-Serrano, S. M.; Lopez-Moreno, J.-I.; Beguería, S.; Lorenzo-Lacruz, J.; Sanchez-Lorenzo, A.; García-Ruiz, J. M.; Espejo, F.: *Evidence of increasing drought severity caused by temperature rise in southern Europe*, Environmental Research Letters, 9(4), 1–9, http://doi.org/10.1088/1748-9326/9/4/044001, (2014a).

Wang, Y.-C.; Hsu, H.-H.; Chen, C.-A.; et al.: *Performance of the Taiwan Earth System Model in Simulating Climate Variability Compared with Observations and CMIP6 Model Simulations*, ESS Open Archive, December 10, 2020, 10.1002/essoar.10505286.1, (2020).

Wilhite, Donald A.; Glanz, Michael H.: *Understanding the Drought Phenomenon: The Role of Definitions*, Drought Mitigation Center Faculty Publications, 20, http://digitalcommons.unl.edu/droughtfacpub/20, (1985).